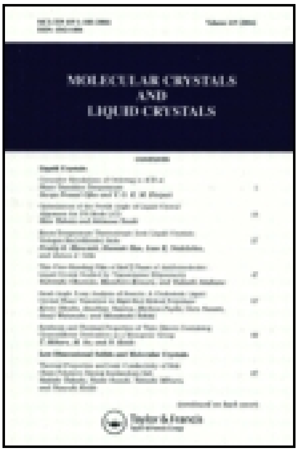

Molecular Crystals and Liquid Crystals Science and Technology. Section A. Molecular Crystals and Liquid Crystals
Publication details, including instructions for authors and subscription information:
http://www.tandfonline.com/loi/gmcl19

Splay Stripes in Hybrid Aligned Nematics with Bulk Elastic Isotropy: The Role of K_{24}

A. Sparavigna [a] & A. Strigazzi [a]
[a] Dipartimento di Fisica, Politecnico di Torino, CISM and INFM, Unità di Torino, C. so Duca degli Abruzzi, 24-0129, Torino, Italy
Version of record first published: 24 Sep 2006.

Mol. Cryst. Liq. Cryst., 1992, Vol. 221, pp. 109–119
Reprints available directly from the publisher
Photocopying permitted by license only

Printed in the United States of America

Splay Stripes in Hybrid Aligned Nematics with Bulk Elastic Isotropy: The Role of K_{24}

A. SPARAVIGNA and A. STRIGAZZI

Dipartimento di Fisica, Politecnico di Torino, CISM and INFM, Unità di Torino, C.so Duca degli Abruzzi, 24 I-10129 Torino (Italy)

(Received December 30, 1990; in final form June 30, 1991)

In hybrid aligned nematic layers a periodic deformation of splay-type may occur at convenient cell thicknesses, if the energetic cost for a mixed twist-splay distortion is less than the cost of a pure splay. In the case of bulk elastic isotropy, we have found that the periodic instability is forbidden, unless the torsional anchoring at the homeotropic substrate is considerably weak. Moreover, the surface-like elastic constant K_{24} is shown deeply to influence the occurrence of the periodic pattern.

I. INTRODUCTION

Recently Lavrentovich and Pergamenshchik[1] reported for the first time the experimental evidence of a periodic instability of splay-type, where close to the distortion threshold a twist is superimposed to the basic splay deformation, occurring in a hybrid aligned nematic (HAN) cell.

In a HAN cell, at the one of the walls the easy direction is homeotropic (H), at the other one it is unidirectional planar (P), due to the surface treatment. If the anchoring is strong, the director **n**, i.e., the local average direction of the molecular axes, is coincident onto each wall with the easy direction; whereas, if the anchoring is weak, the actual **n**-position at one wall is dependent on the competition between the bulk and the substrate under consideration, i.e., finally between the two surfaces themselves.

Everywhere in the cell, the local director can be defined by means of the polar angle θ and azimuth φ. The polar angle θ (called tilt angle) is the angle between the director and the walls, while the azimuth φ (called twist angle) is the angle between the director projection onto the walls (i.e. onto the $/x, y/$ plane—the z-axis being normal to the walls) and the P-easy direction (i.e., the x-axis direction).

In Figure 1(a), a HAN layer of thickness d is represented, with strong torsional anchoring, and weak tilt anchoring: but the tilt anchoring at the H-wall ($z = 0$) is weaker than the one at the P-wall ($z = d$). This means that the HAN deformation is parallel to the plane $/x, z/$, the twist angle φ being zero in the whole cell; furthermore, the angle $(\pi/2) - \theta_0$ is greater than the angle θ_1 (θ_0, θ_1 being the tilt angles at the H- and at the P-wall, respectively).

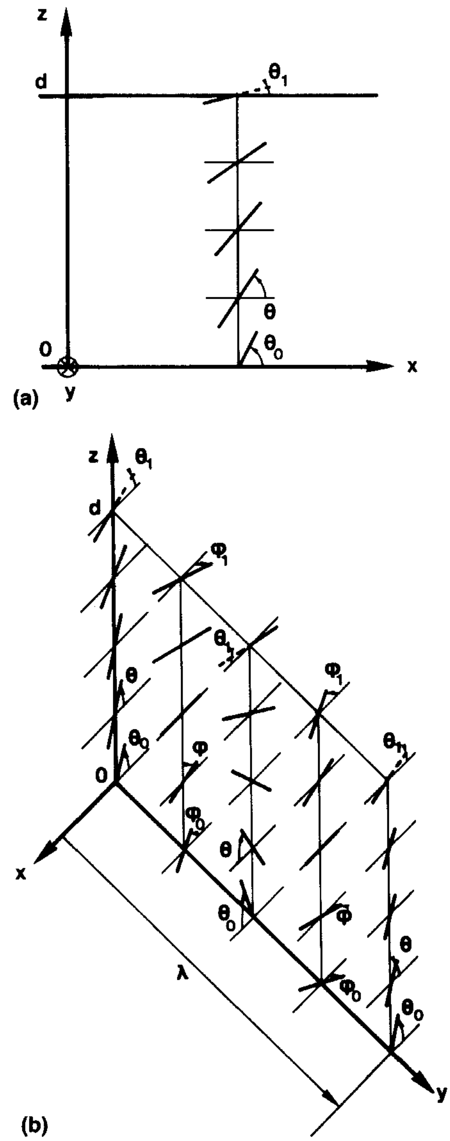

FIGURE 1 Hybrid aligned nematic layer with tilt anchoring strength at the H-wall ($z = 0$) smaller than the one at the P-wall ($z = d$): a) aperiodic distortion in the plane $/xz/$ with tilt angle $\theta(z)$: the twist anchoring is strong at both walls; b) periodic configuration of splay type with tilt angle $\theta(y, z)$ and twist angle $\varphi(y, z)$: also the twist anchoring is weak at both walls.

It is well known,[2] that such an aperiodic HAN deformation can take place, just if the cell thickness is bigger than a threshold value d_a. On the contrary, if $d < d_a$, either the HAN configuration collapses to an undistorted structure governed by the surface with the stronger tilt anchoring, or a periodic deformation (PHAN) takes place, with $\theta(y, z)$ and $\varphi(y, z)$, see Figure 1(b), until another threshold $d_p < d_a$ is reached. Below d_p the undeformed configuration is recomposed.

In Reference 1 the authors described their observations, by supposing the torsional anchoring to vanish; under this restriction, they found by numerical calculation, without linearizing, the threshold d_p of the splay-stripes, i.e. the threshold between PHAN and P configuration, for low values of the elastic ratio $r = K_{22}/K_{11}$ between the twist- and the splay-elastic constant. On the other hand, we studied the occurrence of the splay-stripes in the general case, for whatever weak but finite anchoring[3]: we found that a small decreasing in the twist anchoring at the H-wall has a pronounced effect in favouring the PHAN deformation, enhancing also the critical value r_c, which is the upper limit for the existence of the splay-stripes.

The goal of the present paper is to demonstrate that in the frame of the usual continuum theory[4]: i. the PHAN structure may occur, for conveniently low twist-anchoring energy at the H-wall, also if the twist- and splay-rigidities are identical ($K_{22} = K_{11}$); ii. in this case, the PHAN structure is greatly favoured by the increasing of the ratio between the saddle-splay elastic constant K_{24}[5] and K_{22}, in the range $(-\frac{1}{2}, 1)$, and by the decreasing of the same elastic ratio in the range $(-1, -\frac{1}{2})$.

II. THEORY

Threshold Thickness for Splay Stripes

By assuming $K_{22} = K_{11} \equiv K$, the reduced free energy of a cell portion having thickness d, lengths d_x along the x-axis and λ along the y-axis, where λ is the twist deformation wavelength, has to be defined as $G \equiv 2F/(Kd_x)$, F being the free energy of the same cell portion. Hence

$$G = \int_0^\lambda dy \int_0^d g_b \, dz + G_s \tag{1}$$

where g_b is the bulk kernel and G_s is the surface contribution.

Close to the threshold thickness d_p for periodic instability, by linearizing we have:

$$g_b = (\dot{\varphi}_y + \dot{\theta}_z)^2 + (\dot{\theta}_y - \dot{\varphi}_z)^2 \tag{2}$$

where the dot means the derivative with respect either to y, or to z, according to the corresponding subscript.

The surface contribution, taking into account both anchoring and surface-like elasticity, is given by:

$$G_s = \int_0^\lambda \{L_{\varphi 0}^{-1}\varphi_0^2 - L_{\theta 0}^{-1}\theta_0^2 + L_{\varphi 1}^{-1}\varphi_1^2 + L_{\theta 1}^{-1}\theta_1^2 + 2(1 + \kappa) \cdot [\theta_0\dot{\varphi}_{y0} - \varphi_0\dot{\theta}_{y0} - \theta_1\dot{\varphi}_{y1} + \varphi_1\dot{\theta}_{y1}]\} \, dy \tag{3}$$

where $L_{ij} \equiv K/W_{ij}$ $(i = \varphi, \theta; j = 0, 1)$ are de Gennes-Kléman extrapolation lengths,[6] relevant to the walls $z = 0$, $z = 1$, respectively, W_{ij} being the corresponding anchoring strengths,[7] while $\kappa \equiv K_{24}/K$, as defined. Note that K_{24} is considered as independent of the difference $K_{11} - K_{22}$, as pointed out by Ericksen.[8]

According to the usual procedure, the Euler-Lagrange equation (EL) read

$$\begin{cases} \ddot{\theta}_{yy} + \ddot{\theta}_{zz} = 0 \\ \ddot{\varphi}_{yy} + \ddot{\varphi}_{zz} = 0 \end{cases} \tag{4}$$

We note that EL equations are symmetrical with respect to (y, z), identical with respect to the unknown (θ, φ), and uncoupled. Just the boundary conditions give the coupling between $\theta(y, z)$ and $\varphi(y, z)$, ensuring the orthogonality in y. In fact the boundary conditions, giving the torque equilibrium at the surfaces, are[9]:

$$\begin{cases} R\dot{\theta}_{y0} + L_{\varphi 0}^{-1}\varphi_0 - \dot{\varphi}_{z0} = 0 \\ R\dot{\varphi}_{y0} + L_{\theta 0}^{-1}\theta_0 + \dot{\theta}_{z0} = 0 \\ R\dot{\theta}_{y1} - L_{\varphi 0}^{-1}\varphi_1 - \dot{\varphi}_{z1} = 0 \\ R\dot{\varphi}_{y1} + L_{\theta 1}^{-1}\theta_1 + \dot{\theta}_{z1} = 0 \end{cases} \tag{5}$$

where $R \equiv 1 - 2(1 + \kappa)$.

The solutions of EL equations (4) are periodic with respect to y, and are obtained as:

$$\begin{cases} \theta = (C_1 sh\beta z + C_2 ch\beta z)\cos \beta y \\ \varphi = (C_1' sh\beta z + C_2' ch\beta z)\sin \beta y \end{cases} \tag{6}$$

where $\beta \equiv 2\pi/\lambda$ is the wave number of the splay stripes characterizing the PHAN structure.

By inserting (6) into the boundary conditions (5), with the aim of avoiding trivial solutions, the coefficient determinant D must be zero, D being given by

$$D = \begin{vmatrix} \beta R L_{\varphi 0} & -1 & 0 & \beta L_{\varphi 0} \\ 1 & \beta R L_{\theta 0} & \beta L_{\theta 0} & 0 \\ \beta R L_{\varphi 1} C & C + \beta L_{\varphi 1} S & \beta R L_{\varphi 1} S & S + \beta L_{\varphi 1} C \\ C + \beta L_{\theta 1} S & \beta R L_{\theta 1} C & S + \beta L_{\theta 1} C & \beta R L_{\theta 1} S \end{vmatrix} \tag{7}$$

where $C \equiv ch\beta d$, $S \equiv sh\beta d$.

The equation $D = 0$ implicitly provides the cell thickness d as a function d^* of the wavenumber β, of the anchoring energies, and of the elastic ratio κ. The minimum d_p of such a function vs. β is relevant to the threshold condition for the arising of periodic pattern: the PHAN deformation occurs only for $d > d_p$.

Just some words are to be spent for what is concerning the stability of the periodic solutions: by substituting (6) in the bulk energy density (2) and in the surface energy (3) we can calculate the reduced distortion energy (1) of the cell unit as a function G of the four integration constants C_1, C_2, C_1', C_2'. By applying the minimum condition for G, the vanishing of the first derivatives of G with respect to the integration constants simply provides the homogeneous system relevant to the found equation $D = 0$, giving $d = d^*(\beta)$ again. Moreover, all the four principal minors of the matrix build with the second order derivatives of G with respect to the integration constants are positive for $d = d^*(\beta)$ except to the matrix determinant, which becomes zero in this case, due to the threshold condition. This means that the actual threshold d_p for PHAN, being the minimum of the curve $d = d^*(\beta)$, corresponds to a minimum energy condition, no matter are the values of the anchoring and of the material parameters.

Now the question could arise, what is the actual role of the saddle-splay elasticity? Does it perhaps favour the occurrence of periodic pattern? In order to find the answer, it is necessary to search for the dependence of d_p on κ. Note that, due to the structure of the determinant (7), the threshold thickness d_p is given as a function of R^2, yielding symmetrical results with respect to $R = 0$: as a consequence, $d_p(\kappa)$ is not an even function, being symmetrical with respect to $\kappa = -\frac{1}{2}$. Furthermore, as demonstrated by Ericksen[8] and discussed in Reference 10, for thermodynamical reasons it must be $|\kappa| \leq 1$: this means that R ranges between $(-3, 1)$, being $R = 1$ if $\kappa = -1$, i.e. if K_{24} has no effect at all.

In Figure 2 the behaviour of $d_p(|R|)$ is shown, in the case of strong anchoring of the P-wall ($L_{\theta 1} = L_{\varphi 1} = 0$), for different values of the twist anchoring strength at the H-wall, $L_{\varphi 0}$ ranging from 0.5 μm to 10 μm. Figure 2(a) is relevant to the case $L_{\theta 0} = d_a = 1$ μm, whereas Figure 2(b) is corresponding to the case $L_{\theta 0} = d_a = 5$ μm. We may see that for a given value of the twist anchoring at the H-wall, the PHAN distortion is favoured by increasing values of $|R|$. This may be expected, since the equilibrium of the torques at the walls (5) shows that the surface distortion torque, proportional to R, must balance the anchoring- and the bulk torques: as greater is $|R|$, as smaller can be the surface in-plane periodic deformation, ensuring the same balancing point.

Moreover, starting from strong twist anchoring condition at the H-wall, it is enough a small increasing of $L_{\varphi 0}$ for obtaining a deep enhancing of the PHAN-acceptance area: and this effect is more pronounced if the tilt anchoring at the H-

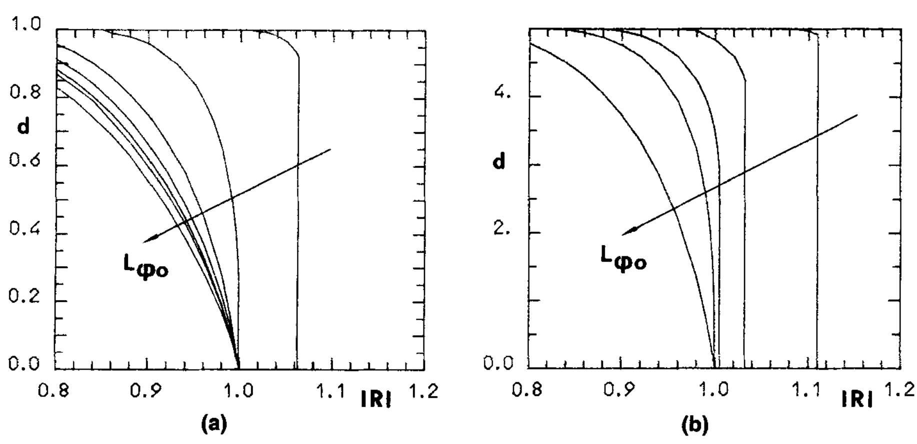

FIGURE 2 Values of the threshold thickness for strong anchoring at the P-wall with a) $L_{\theta 0} = 1$ μm and $L_{\varphi 0}$ having the following values: 0.5, 1, 2, 3, 4, 5, 10 μm; b) $L_{\theta 0} = 5$ μm and $L_{\varphi 0}$ with the following values: 2, 3, 4, 5, 10 μm.

wall is stronger. In fact, in this case the HAN structure should have a bigger splay energetic cost, and consequently it must be unfavoured.

On the other hand, by weakening the surface constraint at the *P*-wall, and considering first a weak twist anchoring ($L_{\varphi 1}$ = 5 μm), for the same values of the other parameters a great enhancing of the PHAN-acceptance area is obtained, with respect to the case considered in Figure 2: and this effect is more pronounced if the tilt anchoring strength at the *H*-wall is higher—see Figure 3(a) ($L_{\theta 0} = d_a$ = 1 μm) compared with Figure 3(b) ($L_{\theta 0} = d_a$ = 5 μm).

On the contrary, by weakening just the tilt anchoring at the *P*-wall, we observe a small decreasing of the PHAN-acceptance area with respect to Figure 2, since the splay energetic content becomes smaller: and such a PHAN-hindering effect is higher if the tilt anchoring at the *H*-wall is also weaker, as discussed above–see Figure 4(a) ($L_{\theta 0}$ = 2 μm, $L_{\theta 1}$ = 1 μm) and Figure 4(b) ($L_{\theta 0}$ = 6 μm, $L_{\theta 1}$ = 1 μm).

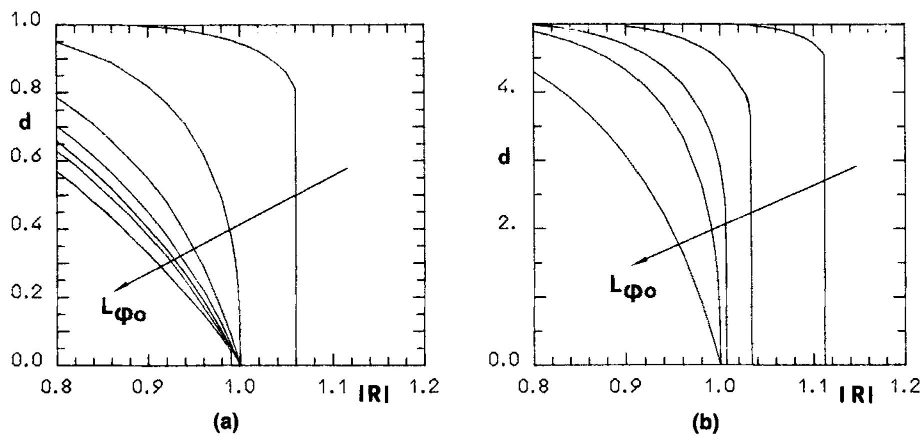

FIGURE 3 Values of the threshold thickness for strong tilt but weak twist anchoring of the *P*-wall, with a) $L_{\theta 0}$ = 1 μm and $L_{\varphi 0}$ = 0.5, 1, 2, 3, 4, 5, 10 μm; b) $L_{\theta 0}$ = 5 μm and $L_{\varphi 0}$ = 2, 3, 4, 5, 10 μm.

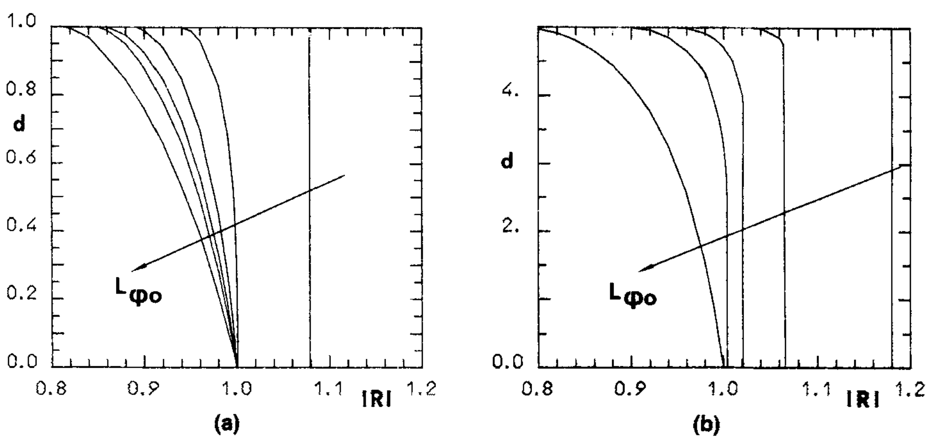

FIGURE 4 Values of the threshold thickness for weak tilt ($L_{\theta 1}$ = 1 μm) but strong twist anchoring at the *P*-wall, with a) $L_{\theta 0}$ = 2 μm and $L_{\varphi 0}$ = 1, 2, 3, 4, 5, 10 μm; b) $L_{\theta 0}$ = 6 μm and $L_{\varphi 0}$ = 2, 3, 4, 5, 10 μm.

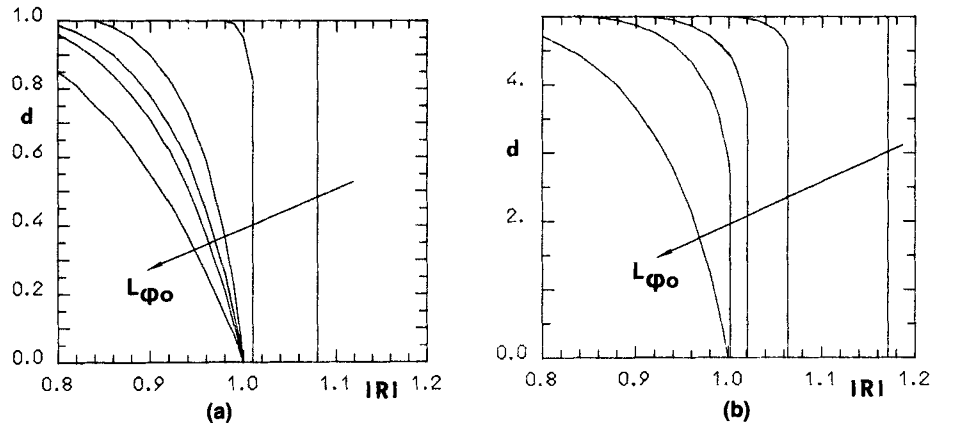

FIGURE 5 Values of the threshold thickness for weak tilt ($L_{\theta 1}$ = 1 μm) and weak twist ($L_{\varphi 1}$ = 5 μm) anchoring at the *P*-wall, with a) $L_{\theta 0}$ = 2 μm and $L_{\varphi 0}$ = 1, 2, 3, 4, 5, 10 μm; b) $L_{\theta 0}$ = 6 μm and $L_{\varphi 0}$ = 2, 3, 4, 5, 10 μm.

Finally, in Figure 5 the behaviour of the PHAN threshold thickness $d_p(|R|)$ is reported, for weak anchoring at both walls, with the previous values of the extrapolation lengths: we conclude that the PHAN configuration is favoured by the increasing of the tilt- and by the diminishing of the twist anchoring strengths.

Are maybe these results dependent on the particular choice of the functional form of the anchoring energy? In order to answer, let us assume a general form $g_{si}[(\psi_i - \Psi_i)^2]$ where $\psi = \theta, \varphi$ and $i = 0, 1$ and Ψ_i is the easy direction at the ith wall.

By expanding g_{si} in power series of $(\psi_i - \Psi_i)^2$, we note that the first term of the expansion corresponds to the Rapini-Papoular form[11]

$$g_{si0} = L_{\psi_i}(\psi_i - \Psi_i)^2 \tag{8}$$

where L_{ψ_i} is the extrapolation length; as usual, such a form has been previously assumed in this paper—see Equation (3). By linearizing, all the other terms than (8) vanish rapidly close to the threshold, which is thus affected just by the first classical term.

How reliable is the linear analysis? Clearly, it holds only close to the threshold, and does not give information on the magnitude of the distortion. But, if the question is actually to calculate thresholds which imply the vanishing of deformation—as in the case of d_p—such kind of analysis turns out to be a simple and powerful tool, allowing to extend the analytical treatment, thus avoiding the possible presence of fictitious solutions, due to the numerical calculation.

Anyway, it is necessary to check the energy behaviour, in order to be sure that the found physical solutions are stable.

Analysis of the Critical Point

It is noticeable that in principle for each given set of the anchoring strengths there exist a critical value $|R_c|$, such as if $|R|$ is less than the critical value itself, the PHAN deformation is forbidden.

In order to determine this critical value, hindering the PHAN structure, let us observe that clearly, $\kappa \to \kappa_c$ implies $\beta \to 0$: thus, by writing extensively the determinant D, after some re-arrangements the factors S and S^2 are to be expanded in series power of β, stopping at the fourth power of the parameter. From (7) we obtain

$$D = D_2\beta^2 + D_4\beta^4 \tag{9}$$

since the zero-th order term and all the odd terms of the expansion identically vanish.

The expansion coefficients D_2, D_4 are given by

$$D_2 = (d + L_{\varphi 0} + L_{\varphi 1})(d - d_a) \tag{10}$$

and by

$$\begin{aligned} D_4 = d\{&R^2[d(L_{\theta 0}L_{\varphi 0} - L_{\theta 1}L_{\varphi 1}) + L_{\theta 0}L_{\theta 1}(L_{\varphi 0} + L_{\varphi 1}) + L_{\varphi 0}L_{\varphi 1}(L_{\theta 0} - L_{\theta 1})] \\ &+ d^3/3 + (2d^2/3)[L_{\varphi 0} + L_{\varphi 1} - (L_{\theta 0} - L_{\theta 1})] - d[(L_{\theta 0} - L_{\theta 1})(L_{\varphi 0} + L_{\varphi 1}) \\ &+ L_{\theta 0}L_{\theta 1} - L_{\varphi 0}L_{\varphi 1}] - L_{\theta 0}L_{\theta 1}(L_{\varphi 0} + L_{\varphi 1}) - (L_{\theta 0} - L_{\theta 1})L_{\varphi 0}L_{\varphi 1}\} \end{aligned} \tag{11}$$

The vanishing of D is ensured by the contemporary vanishing of both D_2 and D_4. The first condition gives $d = d_a$ in the critical point, as may be expected; while the second condition provides the critical value $|R_c|$, obtained as the square root of the relation:

$$\begin{aligned} R_c^2 = [&(d_a^3/3) + (d_a^2/3)(L_{\varphi 0} + L_{\varphi 1}) + L_{\theta 0}L_{\theta 1}(d_a + L_{\varphi 0} \\ &+ L_{\varphi 1})]/[d_a(L_{\theta 0}L_{\varphi 0} - L_{\theta 1}L_{\varphi 1} + L_{\varphi 0}L_{\varphi 1}) + L_{\theta 0}L_{\theta 1}(L_{\varphi 0} + L_{\varphi 1})] \end{aligned} \tag{12}$$

which always is positive if $L_{\theta 0} > L_{\theta 1}$, as in the actual situation concerning just the possibility of splay-stripes.

In particular, in the case of strong anchoring at the P-wall, R_c^2 reads:

$$R_c^2 = (L_{\theta 0}/L_{\varphi 0} + 1)/3 \tag{13}$$

whereas, if only the tilt anchoring at the P-wall is strong, then

$$R_c^2 = L_{\theta 0}[L_{\varphi 0}^{-1} + (L_{\theta 0} + L_{\varphi 1})^{-1}]/3 \tag{14}$$

On the other hand, if just the twist anchoring is strong at the P-wall, thus we have

$$R_c^2 = (1 + d_a/L_{\varphi 0})[1 + L_{\theta 1}/L_{\theta 0} + (L_{\theta 1}/L_{\theta 0})^2]/3 \tag{15}$$

Note that in the presence of strong anchoring either for tilt or for twist at the P-wall, if the twist anchoring at the H-wall becomes strong ($L_{\varphi 0} \to 0$), the critical value of R diverges, and the PHAN configuration is forbidden. Instead, just if the anchoring at the P-wall is weak both for tilt and for twist, the PHAN could appear also in the hypothesis of strong twist anchoring at the H-wall ($L_{\varphi 0} = 0$), since in such a case R_c^2 writes

$$R_c^2 = (1 + d_a/L_{\varphi 1})[(L_{\varphi 0}/L_{\theta 1} - 1)^2/3 + L_{\theta 0}/L_{\theta 1}] \tag{16}$$

and $|R_c|$ can be finite. Note that this effect is more pronounced for smaller values of d_a.

Generally, R_c^2 diminishes hyperbolically with $L_{\varphi 0}$, the horizontal asymptote (for $L_{\varphi 0} \to \infty$) remaining positive. The sensitivity of R_c^2 on $L_{\varphi 0}$ is very high close to $L_{\varphi 0} = 0$.

In Figures 6 and 7 the behaviour of $|R_c|$ vs. $L_{\varphi 0}$ is reported for different anchoring conditions.

It is interesting to discuss the behaviour near the critical point of the wave number β, which characterizes the periodic pattern. Let us consider a particular nematic liquid crystal, having a given value $|R| > |R_c|$, so that at certain cell thicknesses the PHAN can occur. Equation (9) provides

$$\beta^2 = -D_2/D_4 \tag{17}$$

close to the critical point $d \sim d_a$, giving $\beta \sim 0$.

Namely, if we limit ourselves to take into account, for the sake of simplicity,

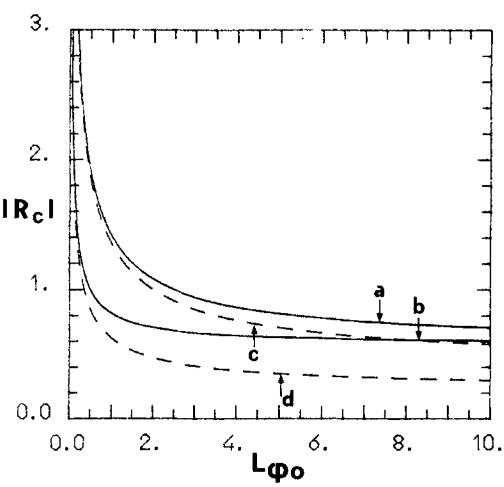

FIGURE 6 Critical values of $|R|$ as a function of $L_{\varphi 0}$. Curves a) and b) refer to the case of strong anchoring at the P-wall (both for tilt and twist) with $L_{\theta 0} = 5$ μm and $L_{\theta 0} = 1$ μm respectively. Curves c) and d) refer to the case of strong tilt but weak twist anchoring ($L_{\varphi 1} = 5$ μm) at the P-wall, with $L_{\theta 0} = 5$ μm and $L_{\theta 0} = 1$ μm respectively.

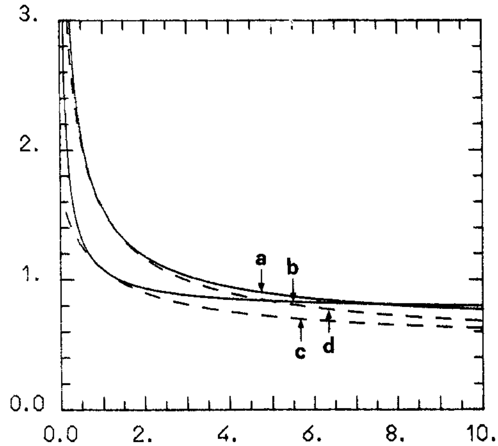

FIGURE 7 Critical values of $|R|$ as a function of $L_{\varphi 0}$. Curves a) and b) refer to the case of strong twist but weak tilt anchoring ($L_{\theta 1}$ = 1 μm) at the P-wall with $L_{\theta 0}$ = 6 μm and $L_{\theta 0}$ = 2 μm respectively. Curves c) and d) refer to the case of weak anchoring at both walls ($L_{\theta 1}$ = 1 μm and $L_{\varphi 1}$ = 5 μm), with $L_{\theta 0}$ = 6 μm and $L_{\theta 0}$ = 2 μm respectively.

only the case of strong anchoring at the one of the wall, where the easy direction is planar, we obtain:

$$\beta^2 = (d_a + L_{\varphi 0})(d_a - d)/\{d_a^3[(R^2 - 1/3)L_{\varphi 0} - d_a/3]\} \tag{18}$$

which means that β vanishes as $(d_a - d)^{1/2}$ close to the critical point. This behaviour is typical of the one occurring in second order transitions.

III. CONCLUSION

The occurrence of static splay stripes in thin nematic layers with opposite tilt boundary conditions was investigated for materials having bulk elastic isotropy. Stable solutions have been found by means of linear analysis, which gives the threshold conditions.

We found that the periodic pattern can appear if the tilt anchoring is weak at the H-wall: but it is necessary the contemporary presence of weak twist anchoring at the H-wall.

In fact, the arising of the splay stripes is deeply favoured by the weakness of the twist anchoring condition of the H-wall: much smaller is the same effect due to the P-wall.

Furthermore, the occurrence of the periodic pattern strongly depends on the value of the elastic ratio $\kappa \equiv K_{22}/K_{22}$: the phenomenon is more favoured when κ becomes smaller in the range $(-1, -\frac{1}{2})$ and greater in the range $(-\frac{1}{2}, 1)$. For any anchoring condition the critical value of κ, hindering the periodic configuration, has been found.

Acknowledgment

This work has been supported by the Ministero dell'Università e della Ricerca Scientifica e Tecnologica of the Italian Government (MURST) and by the Italian Consiglio Nazionale delle Ricerche (CNR) under the research contract No. 90.02149.CT11.

References

1. O. D. Lavrentovich and V. M. Pergamenshchik, *Mol. Cryst. Liq. Cryst.*, **172**, 125 (1990).
2. G. Barbero and R. Barberi, *J. Phys. (France)*, **44**, 609 (1983).
3. A. Sparavigna, L. Komitov, B. Stebler and A. Strigazzi, *Mol. Cryst. Liq. Cryst.*, (1991) **207**, 265 (1991).
4. G. Barbero, A. Sparavigna and A. Strigazzi, *Nuovo Cimento D*, **12**, 1259 (1990).
5. J. Nehring and A. Saupe, *J. Chem. Phys.*, **54**, 337 (1971); **56**, 5527 (1972).
6. P. G. de Gennes, *The Physics of Liquid Crystals* (Clarendon Press, Oxford, 1974); M. Kleman, *Points, Lignes, Parois* (Ed. Physique, Paris, 1977).
7. H. Yokoyama, *Mol. Cryst. Liq. Cryst.*, **165**, 265 (1988) and references therein.
8. J. L. Ericksen, *Arch. Rat. Mech. Anal.*, **9**, 371 (1962); *Phys. Fluids*, **9**, 1205 (1966).
9. V. Smirnov, *Cours de Mathématiques Supérieures*, **IV** (MIR, Moscow, 1975).
10. L. Longa, D. Monselesan and H. R. Trebin, *Liq. Cryst.*, **2**, 769 (1987).
11. G. Barbero and G. Durand, *J. Phys. (France)*, **47**, 2129 (1986).